Downloaded from orbit.dtu.dk on: May 05, 2023

DTU Library

Experimental validation of sound field control with a circular double-layer array of loudspeakers.

Chang, Jiho; Jacobsen, Finn

Published in:
Acoustical Society of America. Journal

Link to article, DOI:
10.1121/1.4792486

Publication date:
2013

Document Version
Publisher's PDF, also known as Version of record

Link back to DTU Orbit

Citation (APA):
Chang, J., & Jacobsen, F. (2013). Experimental validation of sound field control with a circular double-layer array of loudspeakers. *Acoustical Society of America. Journal*, *133*(4), 2046. https://doi.org/10.1121/1.4792486

General rights
Copyright and moral rights for the publications made accessible in the public portal are retained by the authors and/or other copyright owners and it is a condition of accessing publications that users recognise and abide by the legal requirements associated with these rights.

- Users may download and print one copy of any publication from the public portal for the purpose of private study or research.
- You may not further distribute the material or use it for any profit-making activity or commercial gain
- You may freely distribute the URL identifying the publication in the public portal

If you believe that this document breaches copyright please contact us providing details, and we will remove access to the work immediately and investigate your claim.

Experimental validation of sound field control with a circular double-layer array of loudspeakers

Ji-Ho Chang[a] and Finn Jacobsen
Acoustic Technology, Department of Electrical Engineering, Technical University of Denmark, Building 352, DK-2800 Kongens Lyngby, Denmark

(Received 24 September 2012; revised 31 January 2013; accepted 4 February 2013)

This paper is concerned with experimental validation of a recently proposed method of controlling sound fields with a circular double-layer array of loudspeakers [Chang and Jacobsen, J. Acoust. Soc. Am. **131**(6), 4518–4525 (2012)]. The double-layer of loudspeakers is realized with 20 pairs of closed-box loudspeakers mounted back-to-back. Source strengths are obtained with several solution methods by modeling loudspeakers as a weighted combination of monopoles and dipoles. Sound pressure levels of the controlled sound fields are measured inside and outside the array in an anechoic room, and performance indices are calculated. The experimental results show that a method of combining pure contrast maximization with a pressure matching technique provides only a small error in the listening zone between the desired and the reproduced fields, and at the same time reduces the sound level in the quiet zone as expected in the simulation studies well above the spatial Nyquist frequency except at a few frequencies. It is also shown that errors in the positions of the loudspeakers can be critical to the results at frequencies where the distance between the inner and the outer array is close to half a wavelength. © *2013 Acoustical Society of America*.
[http://dx.doi.org/10.1121/1.4792486]

PACS number(s): 43.38.Md, 43.38.Vk [MRB] Pages: 2046–2054

I. INTRODUCTION

Recent studies have attempted to provide simultaneously a sound field that imitates a desired one inside a circular or a spherical array of loudspeakers and a quiet zone outside the array.[1–5] These systems can have two advantages: one is to reduce the effect of reflections from a room so as to improve the degradation of sound quality due to the reflections. The other is to prevent other people outside the array from hearing the sound from the loudspeakers, which can be useful either if the sound contains confidential information, or if it is disturbing.

Methods to control an interior and exterior field have been proposed that use loudspeakers of first-order fixed or variable directivities in two-dimensional (2D) and 3D cases.[1–3] These methods interpret continuous monopole and dipole sources on the boundary of a region in the Kirchhoff–Helmholtz integral equation as discrete loudspeakers of first-order directivity that can be modeled with monopoles and dipoles. Another study has shown that more accurate reproduction is possible with higher-order variable directivity sources in the 2D case.[4] On the other hand, a method with a circular double-layer of loudspeakers has been proposed in the 2.5D case, which interprets the monopoles and dipoles as a double-layer of loudspeakers without assuming that the directivity of the loudspeakers can be controlled.[5] These studies, however, have been based on theoretical studies and computer simulations, and no experimental validation has been provided.[1–5]

For experimental validation of sound field control, the effects of errors in transfer functions between the source strengths and the sound fields have been studied,[6,7] and regularization methods have been discussed and proposed to improve the degradation due to the errors.[7–9] However, these studies have also exclusively been based on computer simulations. On the other hand, only a few studies that validate sound field control with loudspeakers experimentally have been published.[10–15] These studies have shown that the sound field control is feasible as expected from the simulations, but the exterior region of the loudspeakers array has not been considered.

The objective of this paper is to present and discuss experimental validation of sound field control with a circular double-layer of loudspeakers proposed in a previous study.[5] The double-layer of loudspeakers is realized with 20 pairs of closed-box loudspeakers that are mounted back-to-back. The loudspeakers are modeled as a combination of monopoles and dipoles, and source strengths of pure tones are obtained with several solution methods. The generated sound fields are measured inside and outside the array in an anechoic room with a microphone array, and performance indices are calculated. In addition, errors in the positions of loudspeakers and the effects of regularization are discussed.

II. EXPERIMENTAL SETUP

A. The loudspeaker array, the listening zone, and the quiet zone

Figure 1 shows a circular double-layer array of the loudspeakers that is used for this experiment. Each pair is composed of two closed-box loudspeakers mounted back-to-back. The enclosure size of each one is 10 cm

[a]Author to whom correspondence should be addressed. Current address: Center for Applied Hearing Research, Department of Electrical Engineering, Technical University of Denmark, DK-2800 Kgs. Lyngby, Denmark. Electronic mail: chang.jiho@gmail.com

Downloaded 16 Apr 2013 to 192.38.67.112. Redistribution subject to ASA license or copyright; see http://asadl.org/terms

FIG. 1. (Color online) The loudspeaker array in the anechoic room.

(width) × 10 cm (height) × 15 cm (depth), and thus the depth of each pair is 30 cm. The inner and the outer array are composed of 20 loudspeakers facing inward and outward, respectively. The loudspeakers are located on a ring of radius 1.5 m as illustrated in Fig. 2. The distances from the center of the circle to the baffle planes of the inner loudspeakers and those of the outer loudspeakers are 1.35 and 1.65 m, respectively. Errors in the positions of loudspeakers are approximately within 2 cm.

The listening zone S_b is defined as a circular region located in the plane of the circles inside the array, and the radius is 0.2 m considering the size of the head of a listener. The quiet zone S_d is a ring-shaped region outside the array, and the radius of the inner circle of the quiet zone (r_d) is 2.5 m, and the width (Δr_d) is 1 m. The listening and the quiet zones are sampled at discrete points: $\vec{r}_b^{(1)}, \vec{r}_b^{(2)}, \ldots, \vec{r}_b^{(M_b)}$ and $\vec{r}_d^{(1)}, \vec{r}_d^{(2)}, \ldots, \vec{r}_d^{(M_d)}$. Thus, the sound pressure in the zones can be expressed as vectors,

$$\mathbf{P}_b(\omega) = \left[P\left(\vec{r}_b^{(1)};\omega\right) \;\; P\left(\vec{r}_b^{(2)};\omega\right) \;\; \cdots \;\; P\left(\vec{r}_b^{(M_b)};\omega\right) \right]^T, \tag{1}$$

$$\mathbf{P}_d(\omega) = \left[P\left(\vec{r}_d^{(1)};\omega\right) \;\; P\left(\vec{r}_d^{(2)};\omega\right) \;\; \cdots \;\; P\left(\vec{r}_d^{(M_d)};\omega\right) \right]^T, \tag{2}$$

where $P(\vec{r};\omega)$ is the complex pressure at the frequency ω (omitted in what follows for simplicity). The frequency range of interest is between 100 Hz and 1 kHz. The spacing between the adjacent sampling points is 7.5 cm, which is less than 1/4 of the wavelength at the maximum frequency, 1 kHz.

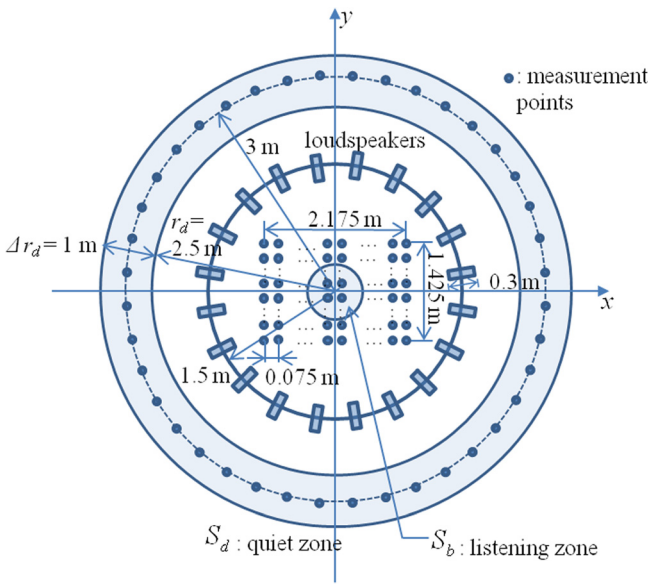

FIG. 2. (Color online) The array of loudspeakers, the listening and the quiet zones, and measurement points inside and outside the loudspeaker array.

The sound field generated by all loudspeakers at a given position can be expressed as

$$P(\vec{r}) = \sum_{n=1}^{40} H\left(\vec{r}|\vec{r}_s^{(n)}\right) q^{(n)}, \tag{3}$$

where $q^{(n)}$ is the complex source strength of the nth loudspeaker, and $H(\vec{r}|\vec{r}_s^{(n)})$ is the transfer function between the nth source strength and the sound pressure at $\vec{r}$. Each loudspeaker is independently driven by the corresponding source strength, and the source strengths are defined as the analog signals that are generated by sound cards. Thus, the unit of $q^{(n)}$ is volt [V], and that of $H(\vec{r}|\vec{r}_s^{(n)})$ is [Pa/V].

Equation (3) can be written in matrix form for $\mathbf{P}_b$ and $\mathbf{P}_d$,

$$\mathbf{P}_b = \mathbf{H}_b \mathbf{q}, \tag{4}$$

$$\mathbf{P}_d = \mathbf{H}_d \mathbf{q}, \tag{5}$$

where

$$\mathbf{H}_b = \begin{bmatrix} H\left(\vec{r}_b^{(1)}|\vec{r}_s^{(1)}\right) & \cdots & H\left(\vec{r}_b^{(1)}|\vec{r}_s^{(40)}\right) \\ \vdots & \ddots & \vdots \\ H\left(\vec{r}_b^{(M_b)}|\vec{r}_s^{(1)}\right) & \cdots & H\left(\vec{r}_b^{(M_b)}|\vec{r}_s^{(40)}\right) \end{bmatrix}, \tag{6}$$

$$\mathbf{H}_d = \begin{bmatrix} H\left(\vec{r}_d^{(1)}|\vec{r}_s^{(1)}\right) & \cdots & H\left(\vec{r}_d^{(1)}|\vec{r}_s^{(40)}\right) \\ \vdots & \ddots & \vdots \\ H\left(\vec{r}_d^{(M_d)}|\vec{r}_s^{(1)}\right) & \cdots & H\left(\vec{r}_d^{(M_d)}|\vec{r}_s^{(40)}\right) \end{bmatrix}, \tag{7}$$

$$\mathbf{q} = \left[q^{(1)} \;\; q^{(2)} \;\; \cdots \;\; q^{(40)} \right]^T. \tag{8}$$

Sound pressure at $\vec{r}$ in the desired field is denoted as $\hat{P}(\vec{r})$, and the sound pressure at discrete points in the listening zone and the quiet zone can be expressed as vectors, $\hat{\mathbf{P}}_b$ and $\hat{\mathbf{P}}_d$. According to the objective, $\hat{\mathbf{P}}_d$ is a zero-vector (M_d by 1). For simplicity, the desired field is a plane wave with an amplitude of B propagating in the negative x-direction,

$$\hat{P}(r,\phi) = \begin{cases} Be^{-ikr\cos(\phi-\pi)}, & r < r_b \\ 0, & r_d < r < r_d + \Delta r_d, \end{cases} \tag{9}$$

where B is the magnitude and ϕ is the azimuth angle. The magnitude B is chosen to be 0.05 Pa considering the signal-to-noise ratio and output ranges of the loudspeakers,

Downloaded 16 Apr 2013 to 192.38.67.112. Redistribution subject to ASA license or copyright; see http://asadl.org/terms

and thus the sound pressure level is 68 dB sound pressure level.

B. Loudspeaker modeling

In order to obtain the source strengths $\mathbf{q}$, the transfer functions, $\mathbf{H}_b$ and $\mathbf{H}_d$, need to be measured or modeled. Measurements of transfer functions provide more accurate information, but they require too much effort to be used in practice. To avoid this problem, each loudspeaker is modeled as a weighted combination of a monopole and a dipole oriented in the radial direction. This model is valid in the frequency range of interest because loudspeakers behave as monopoles at low frequencies where the wavelengths are longer than the dimensions of the loudspeakers, and the dipole term can express directivities of the loudspeakers at higher frequencies. The transfer function can be expressed as

$$H\left(\vec{r}|\vec{r}_s^{(n)}\right) = \nu\frac{A^{(n)}e^{-ikR^{(n)}}}{R^{(n)}} + (1-\nu)\frac{A^{(n)}e^{-ikR^{(n)}}}{R^{(n)}}\left(1-\frac{i}{kR^{(n)}}\right)\cos\theta_s^{(n)}, \tag{10}$$

where ν is a weighting parameter ($0 \le \nu \le 1$), $R^{(n)} = |\vec{r}_s^{(n)} - \vec{r}|$, and $\theta_s^{(n)}$ is the angle between the axis of the dipole and the observation point, k is the wave number, and $A^{(n)}$ is the complex magnitude of the transfer function [Pa m/V].

The position of the center $\vec{r}_s^{(n)}$ and the parameter ν are experimentally determined so as to reduce the averaged spatial error between the modeled and the measured transfer functions. That is, the transfer functions of a loudspeaker are measured in the front and back regions of the loudspeaker, and compared with monopoles at various positions in the center by calculating the normalized spatial error between them. Figure 3 (left) shows the magnitudes of the transfer functions at 100 Hz where the solid and the dotted lines indicate the enclosure of the active loudspeaker facing the $+y$ direction (inward) and that of the inactive loudspeaker facing the $-y$ direction (outward), respectively. The center position of this pair is at $(-1.5\,\text{m}, 0)$. Figure 3 (right) shows the normalized spatial errors between the measured and the modeled transfer function at 100 Hz where each grid is the position of the monopole. The dotted line shows the loudspeaker enclosure, and the white $\times$ indicates the position with the minimum error.

Even if the position that has the minimum error varies with frequency, the error has the minimum when the center is located around 5 cm in front of the center of the baffle plane at all frequencies of interest on the assumption that $\nu = 1$. This shift to front shows that the center of the spherical wave is located in front of the driver, which is called the acoustic center.[16,17] Hence, the position of the center $\vec{r}_s^{(n)}$ was determined first as 5 cm in front of the baffle plane, and then the weighting parameter ν was determined based on the averaged spatial error. As shown in Fig. 4, the modeling error is reduced by taking a weighting parameter ν that is smaller than 1 above 500 Hz because the directivity of the loudspeakers can be considered. At each frequency, the weighting parameter that has the minimum error is chosen, that is, $\nu = 1$ below 400 Hz, $\nu = 0.9$ at 500 to 900 Hz, and $\nu = 0.8$ at 1 kHz. The modeling error increases with frequency, but it does not exceed -10 dB at any frequency of interest.

The loudspeakers differ by ± 1 dB in magnitude and by $\pm 10°$ in phase. These differences are compensated by obtaining $A^{(n)}$ of each loudspeaker. The speed of sound is estimated to be 345 m/s from the temperature and the humidity in the anechoic room.

The other loudspeakers are assumed to have the acoustic centers in 5 cm front of the baffled planes. Hence, the distances to the acoustic centers of the inner and the outer arrays are 1.30 and 1.70 m because the distances to the baffle planes are 1.35 and 1.65 m as explained in Sec. II A. That is, the position of the nth loudspeaker in polar coordinates is

$$\left(r_s^{(n)}, \phi_s^{(n)}\right) = \begin{cases} \left(1.30, 2\pi(n-0.5)/20\right), & n \le 20, \\ \left(1.70, 2\pi(n-20-0.5)/20\right), & 21 \le n \le 40. \end{cases} \tag{11}$$

The spacing between adjacent loudspeakers is 0.408 m on the inner array and 0.440 m on the outer array. The spatial Nyquist frequencies at which the spacing on the inner and

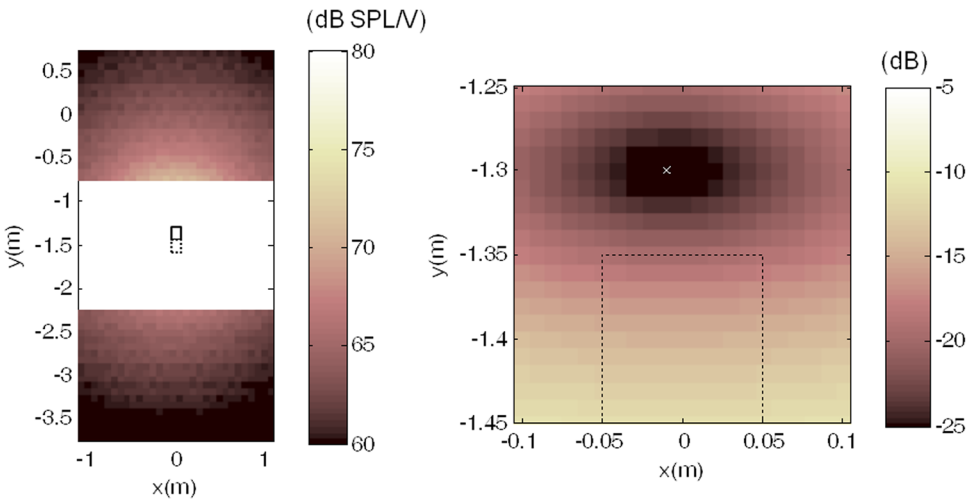

FIG. 3. (Color online) The magnitude of the transfer function of a loudspeaker (left) and the normalized averaged error between the measured and the modeled transfer function with several positions (right). Result at 100 Hz.

Downloaded 16 Apr 2013 to 192.38.67.112. Redistribution subject to ASA license or copyright; see http://asadl.org/terms

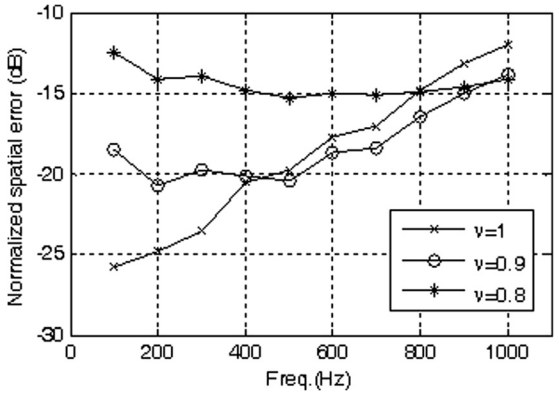

FIG. 4. Normalized spatial error between the measured transfer function and the combined model of a monopole and a dipole as a function of the frequency.

the outer arrays are equal to half a wavelength are 423 and 392 Hz, respectively. It is well known that sound waves can be reproduced below the spatial Nyquist frequency.[18]

C. Solution methods

Several solution methods have been suggested to optimize two performance indices at the same time in the previous study. One of the indices is the acoustic contrast, which is defined as the ratio of the average acoustic potential energy density in the listening zone to that in the quiet zone.[19] In discrete form, this ratio becomes

$$\mu = \frac{M_d}{M_b}\frac{\mathbf{P}_b{}^H\mathbf{P}_b}{\mathbf{P}_d{}^H\mathbf{P}_d}, \tag{12}$$

where the superscript H indicates the Hermitian transpose. The other performance index is the normalized spatial average error between the desired and the reproduced field in the listening zone, defined as

$$\bar{e}_b = \frac{(\hat{\mathbf{P}}_b - \mathbf{P}_b)^H(\hat{\mathbf{P}}_b - \mathbf{P}_b)}{\hat{\mathbf{P}}_b{}^H\hat{\mathbf{P}}_b}. \tag{13}$$

The solution that maximizes the acoustic contrast is obtained as the eigenvector corresponding to the maximum eigenvalue of the matrix $\mathbf{R}_d{}^{-1}\mathbf{R}_b$, as follows:

$$[\mathbf{R}_d{}^{-1}\mathbf{R}_b]\mathbf{q}_{ct} = \mu_{\max}\mathbf{q}_{ct}, \tag{14}$$

where $\mathbf{R}_d = \mathbf{H}_d{}^H\mathbf{H}_d/M_d$ and $\mathbf{R}_b = \mathbf{H}_b{}^H\mathbf{H}_b/M_b$. The magnitude of the solution is normalized such that

$$(\mathbf{H}_b\mathbf{q}_{ct})^H(\mathbf{H}_b\mathbf{q}_{ct}) = \hat{\mathbf{P}}_b{}^H\hat{\mathbf{P}}_b. \tag{15}$$

On the other hand, the solution that combines pure contrast maximization with a pressure matching technique has been proposed as follows:[5]

$$\mathbf{q}_{cb} = [\kappa\mathbf{H}_d{}^H\mathbf{H}_d + (1-\kappa)\mathbf{H}_b{}^H\mathbf{H}_b]^{-1}(1-\kappa)\mathbf{H}_b{}^H\mathbf{P}_b, \tag{16}$$

where κ $(0 \le \kappa < 1)$ is a weighting factor that determines the balance between the potential energy in the quiet zone and the mean square error in the listening zone. As κ approaches 1, the solution tends to minimize the acoustic potential energy in the quiet zone, and as κ approaches 0, the solution tends to minimize the error in the listening zone. The solution is equivalent to the least-square solution if κ is 0.5. The solutions are regularized in the same way as in the previous paper,[5] which is based on the truncated singular value decomposition and the discrepancy principle.[20] The effect of regularization is discussed in Sec. IV.

D. Measurement setup

A planar array of 30×20 microphones is used to measure the controlled sound fields in the listening zone. As illustrated in Fig. 2, the measurement region inside the array is a rectangle (2.175 m × 1.425 m), which includes the listening zone. The spacing between the adjacent points is 0.075 m.

The sound field outside the array is measured at 40 positions on a circle of radius 3.0 m that is included in the quiet zone as illustrated in Fig. 2. These measurement positions outside the array are different from those used to obtain the source strengths, $\vec{r}_d^{(1)}, \vec{r}_d^{(2)}, \ldots, \vec{r}_d^{(M_d)}$. At each position, the sound pressure is measured along the z-axis with a linear array of microphones to observe the sound propagation in the upward and downward directions. The number of measurement points along z-axis is 24, $z = -0.9$–0.825 m with spacings of 7.5 cm where the plane of interest is in $z = 0$. Thus, the total number of measurement points outside the array is 960 (40×24).

The resultant sound fields are directly measured by generating all loudspeakers with pure tones of the obtained source strengths at each frequency, instead of calculating with Eq. (3).

III. RESULTS

A. Performance in the horizontal plane

Figure 5 shows the sound field obtained with the combined solution ($\kappa = 0.5$) at 200, 500, and 800 Hz from the left to the right. The first and the second rows are the sound pressure level and phase inside the array, respectively. The dotted circle indicates the listening zone. The phase decreases in the negative x-direction in the listening zone, which implies that a plane wave propagates in this direction. The magnitude of the plane wave is about 68 dB as intended at 200 and 500 Hz, but decreases by 10 dB at 800 Hz. The last row is the sound pressure level outside the array. Compared with the level in the listening zone, the difference is approximately 35, 25, and 15 dB at these frequencies, respectively.

When the sound field is obtained with pressure matching in the listening zone ($\kappa = 0$), a plane wave is generated, and the sound pressure level is about 68 dB in the listening zone, and about 40–60 dB in the quiet zone at these frequencies (not shown). On the other hand, in the sound field obtained with contrast control, a plane wave is not generated, and the level is about 68 dB in the listening zone because of the

Downloaded 16 Apr 2013 to 192.38.67.112. Redistribution subject to ASA license or copyright; see http://asadl.org/terms

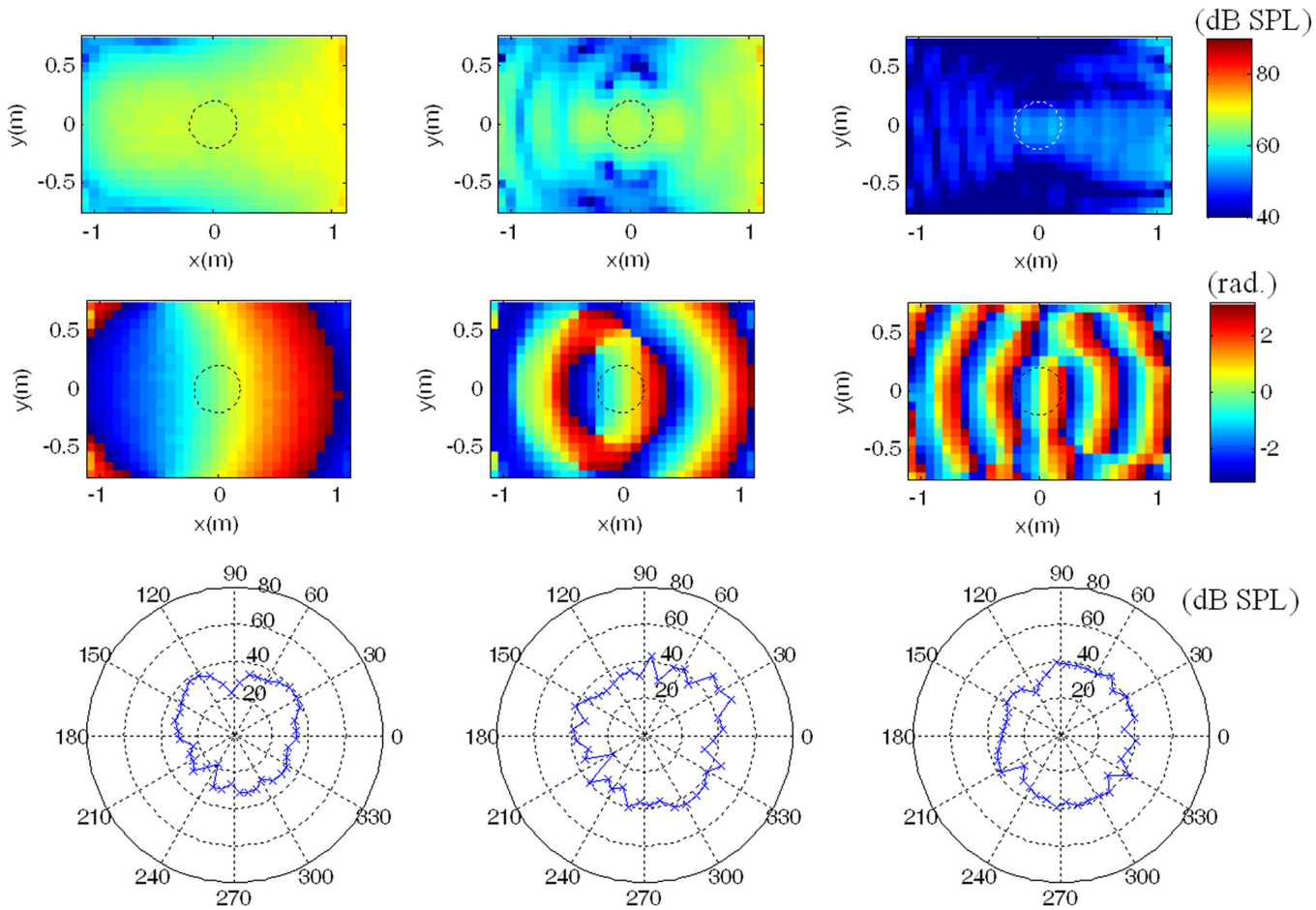

FIG. 5. (Color online) Sound field obtained with pressure matching ($\kappa = 0.5$): First row: sound pressure level inside the array; second row: phase inside the array; third row: sound pressure level outside the array. Results at 200, 500, and 800 Hz from left to right.

normalization [Eq. (15)], and about 20–40 dB in the quiet zone at these frequencies (not shown). Compared with these methods, the combined method (Fig. 5) shows higher contrast than the pressure matching in the listening zone and lower spatial error than the contrast control.

Figure 6 shows a comparison of the two performance indices as functions of frequency obtained with various solutions: contrast control, pressure matching in the listening zone ($\kappa = 0$), and the combined solution with $\kappa = 0.1$, 0.5, and 0.9. This contrast is calculated from the sound pressure at the measurement points in the listening and quiet zones. The maximum contrast is obtained with the contrast control at most frequencies, and pressure matching in the listening zone gives the lowest contrasts at all frequencies. The contrast obtained with the combined solution exceeds 30 dB below the Nyquist frequency of the outer array (392 Hz), and takes higher values than 20 dB up to 700 Hz. On the other hand, the minimum spatial error is obtained with pressure matching in the listening zone ($\kappa = 0$), and the spatial error obtained with contrast control is the largest at all frequencies. The spatial errors obtained with the combined solution are lower than −15 dB below the Nyquist frequency of the outer array, and increase to values from −15 to 0 dB at higher frequencies. The results at 400 Hz show performance degradation, which is discussed in Sec. IV.

B. Performance in the vertical plane

Figure 7 shows the sound field on a cylindrical surface outside the array (φ-z plane, $r = 2.815$ m) at 200 Hz obtained with the combined solution ($\kappa = 0.5$). Even if the sound pressure level is reduced to less than 40 dB around the plane of interest ($z = 0$), this level increases above and below this plane. In particular, the sound pressure at vertically high and low positions takes a higher value at $\varphi = 0$ than other angles where the plane wave is coming from.

IV. DISCUSSION

A. Errors in the positions of the loudspeakers

The contrast and the spatial error in the experimental results (Fig. 6) differ from those in the simulation results obtained in the same condition (Fig. 8) by a maximum of 25 dB up to 500 Hz. For example, as shown in Fig. 8, the contrast with the combined solution ($\kappa = 0.5$) is about 50 dB at 100–300 Hz, and decreases to more than 45 and 30 dB at 400 and 500 Hz, respectively (not shown). This difference can be caused by experimental errors, i.e., positioning errors of loudspeakers, modeling errors, and background noise. Among these errors, the modeling error is estimated to be less than −20 dB below 500 Hz, and −10 dB at 600 Hz–1 kHz (Fig. 4). The background noise is negligible because

Downloaded 16 Apr 2013 to 192.38.67.112. Redistribution subject to ASA license or copyright; see http://asadl.org/terms

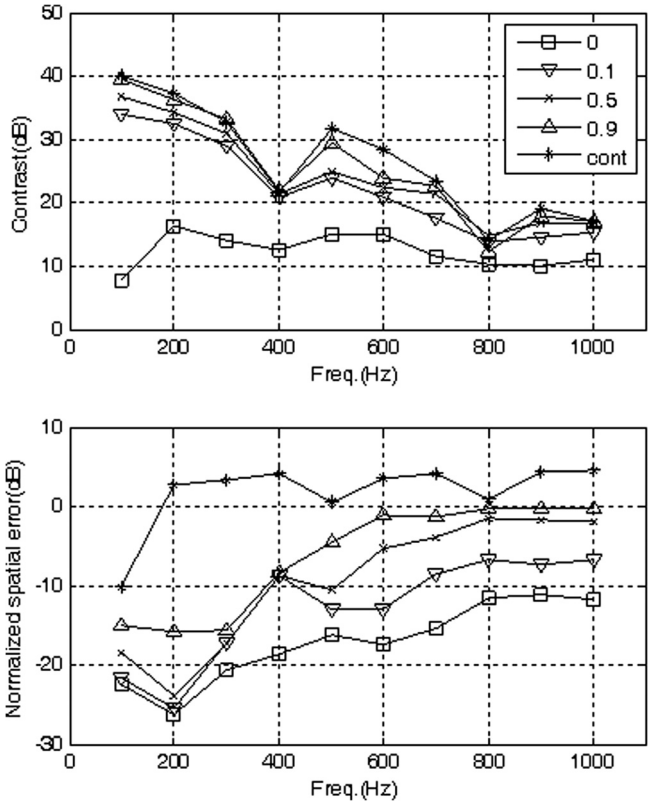

FIG. 6. Acoustic contrast and normalized spatial error in the experiment: contrast control (∗), pressure matching in the listening zone (□), and combined solution with $\kappa = 0.1$ (▽), 0.5 (×), and 0.9 (△).

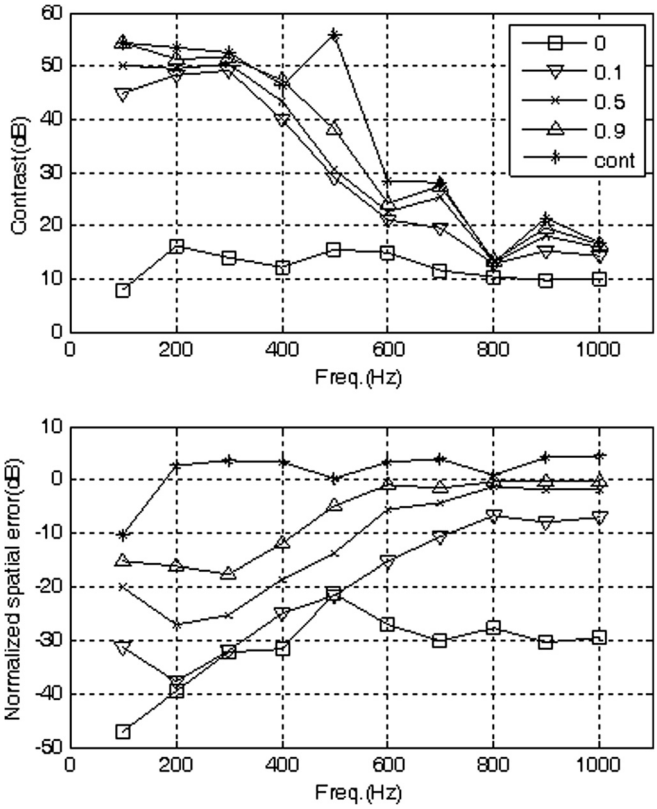

FIG. 8. Acoustic contrast and normalized spatial error in the simulation result with the same condition as the experiment.

the signal-to-noise ratio is more than 20 dB (not shown). The errors in the positions of loudspeakers have been known to be critical to crosstalk cancellation of two loudspeakers systems for stereo.[21]

Figure 9 shows a simulation result obtained by assuming that the distances from the center to the loudspeakers are not identical but have errors from −2 to 2 cm based on the measured diameters of the ring. For simplicity, the error in the tangential direction is assumed to be zero. This result is closer to the experimental results than the simulation result at 100 to 500 Hz, and a large degradation of the performance occurs at 400 Hz. This means that the positioning error of the loudspeakers can be critical and induce a large error at some frequencies.

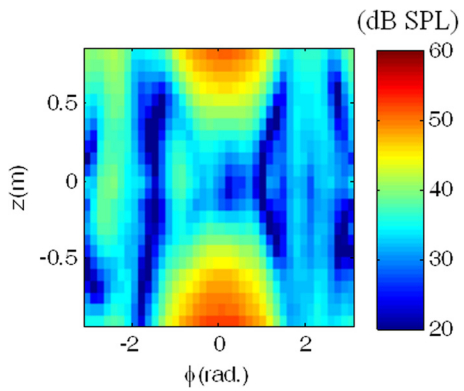

FIG. 7. (Color online) The magnitude of the sound field outside the array at 200 Hz obtained with the combined solution ($\kappa = 0.5$).

Figures 10 shows the vector norms of the source strengths (top) and the condition numbers of the matrices for inversion in Eq. (16) (bottom), respectively. The highest norm is obtained at 400 Hz, which is expected to induce the large effect of the positioning error at 400 Hz. However, this cannot be explained by the condition number because at 400 Hz it is smaller than at 100–300 Hz.

This can be explained with the distance between the inner and the outer array of loudspeakers. The distance 40 cm is close to half-a-wavelength at 400 Hz, 43 cm. This means that each pair of loudspeakers can cancel each other. In the controlled sound field at 400 Hz with the simulation, the sound level in the region between the inner and the outer array is higher than that in the listening region by about 20 dB (not shown). This implies that the cancellation between the loudspeakers is reduced by the positioning error in the experiment, and as a result the sound waves reach the listening and the quiet zones.

B. The effect of regularization

As shown in Fig. 10 (bottom), the matrices are not robust at 100–300 Hz. Even if the positioning errors are expected to have smaller effect because of relatively long wavelengths at these frequencies, the errors can occasionally lead to large errors in the controlled sound field. However, this problem can be reduced with regularization, but it is difficult to determine the optimal regularization parameter without accurate information of the errors if the system has

Downloaded 16 Apr 2013 to 192.38.67.112. Redistribution subject to ASA license or copyright; see http://asadl.org/terms

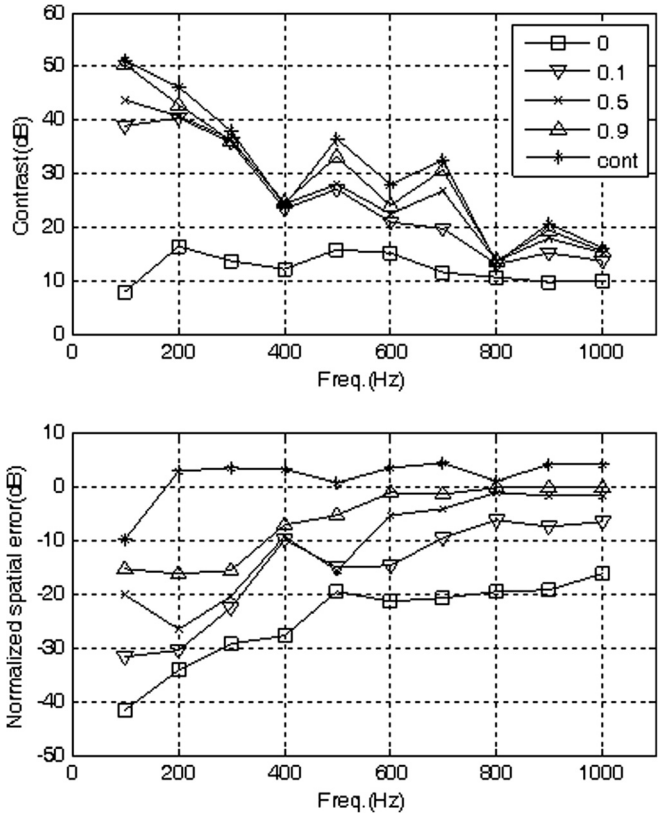

FIG. 9. Acoustic contrast and normalized spatial error in the simulation result with the positioning errors of the loudspeakers.

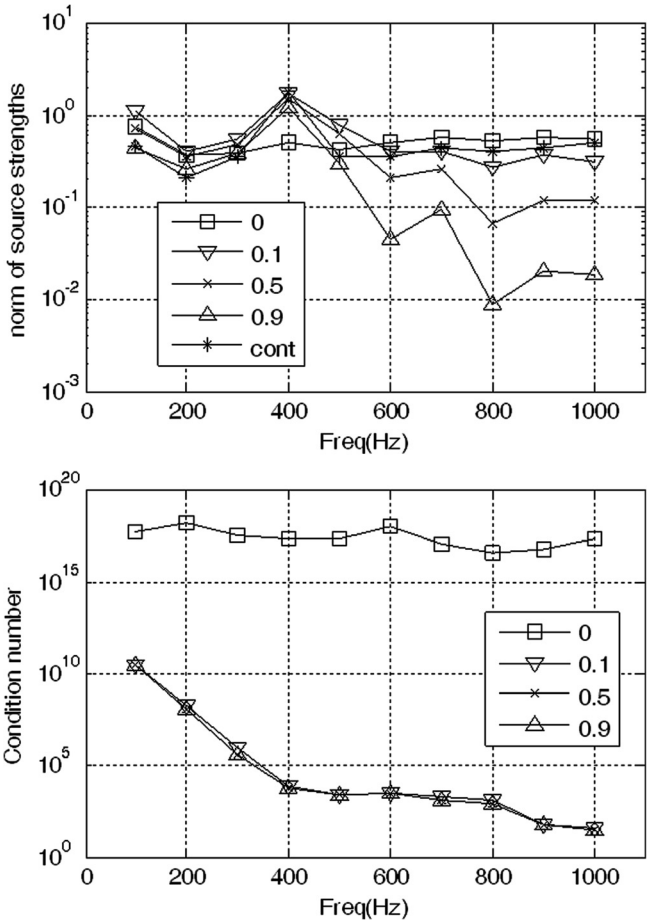

FIG. 10. The vector norms of the source strengths (top) and condition number of the matrices for inversion (bottom).

the error, not the output. For example, the L-curve method has been widely used to determine the optimal regularization parameter, but this method assumes that the output has uncorrelated error,[22,23] and the combined method does not have a distinct corner of the L-curve (not shown).

In order to investigate the effect of regularization, the contrast and the normalized spatial error are obtained in simulations and experiments with various parameters of the Tikhonov regularization method[23] in the case of $\kappa = 0.5$. That is, regularized solutions are used as follows:

$$\tilde{\mathbf{q}}_{cb} = [\mathbf{H}_d{}^H\mathbf{H}_d + \mathbf{H}_b{}^H\mathbf{H}_b + \alpha\mathbf{I}]^{-1}\mathbf{H}_b{}^H\mathbf{P}_b, \tag{17}$$

where α is a regularization parameter. This solution is different from what is used in the previous paper,[5] but it has been well known that Tikhonov regularization produces similar results to the regularization based on the truncated singular value.[22]

Figure 11 shows the contrast and the normalized spatial error obtained with various values of the parameter α, 10^{-2}–10^{2}, in the experiment. The vector norm of the source strengths and the condition number decrease with the parameter (not shown). At most frequencies, the contrast takes the highest value with the parameter 10^{1}, and the spatial error has the lowest value with the parameter 10^{-2}. The contrast is improved by 5 dB at some frequencies, and the spatial error is increased in this case.

Figure 12 shows the simulation results with the same condition as that in Fig. 11 and the positioning errors that are introduced in Fig. 9. This means that perturbed matrices with the positioning errors are used to obtain the reproduced sound field in this simulation. The contrast takes about 35–50 dB at 100–300 Hz with the parameter 10^{-2}–10^{1}. These results are higher than those in the experimental results by about 10 dB at 100 Hz and 5 dB at 200 Hz, and then the differences decrease into less than 5 dB at 300 and 400 Hz. With the regularization parameter 10^{2}, the contrast and the spatial error approach those in the experiment, and the differences are less than 3 and 1 dB, respectively. This means that the regularization makes the solution robust to the experimental error. It is expected that the smaller experimental errors reduce the difference between the experiment and the simulation with the smaller regularization parameter.

C. Vertical propagation

As can be seen in Fig. 7, the sound pressure level out of the plane of interest is higher than that in the plane of interest ($z = 0$), which implies that sound waves propagate upward and downward. These waves need to be acoustically treated with sound absorbing material unless the array is placed under anechoic condition because the waves can be reflected from the ceiling and the floor and affect the sound field in the plane of interest. Nevertheless, in the second case with the combined solution, the sound pressure takes a high value only around $\varphi = 0$. If the direction of the plane wave is

Downloaded 16 Apr 2013 to 192.38.67.112. Redistribution subject to ASA license or copyright; see http://asadl.org/terms

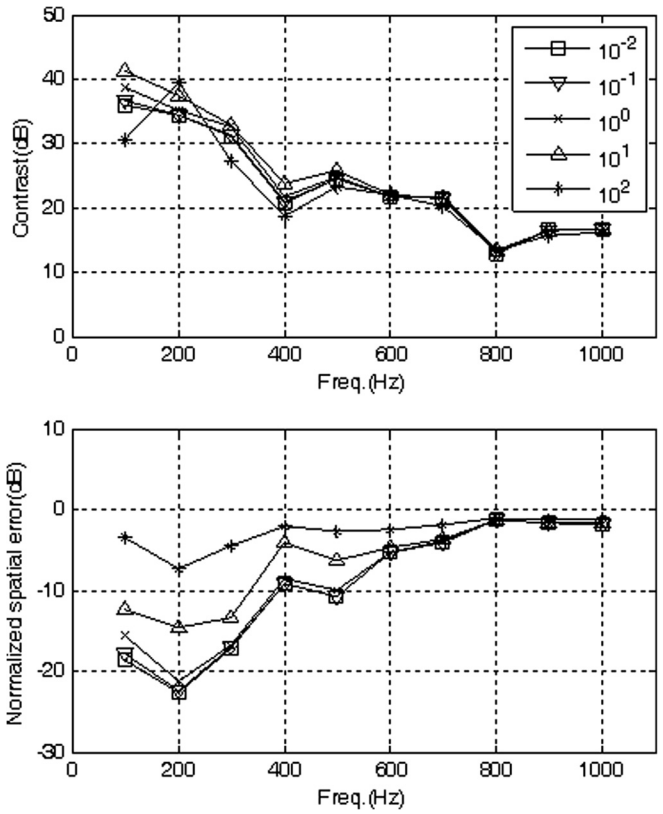

FIG. 11. Acoustic contrast and normalized spatial error in the experiment with several regularization parameters α: 10^{-2} (□), 10^{-1} (▽), 10^{0} (×), 10^{1} (△), and 10^{2} (∗).

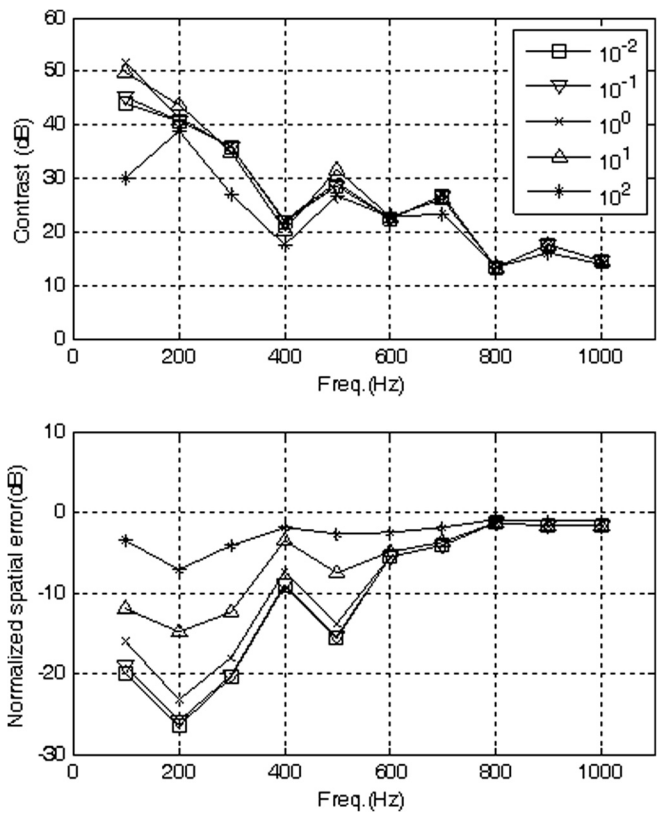

FIG. 12. Acoustic contrast and normalized spatial error in the simulation with the positioning errors of the loudspeakers and several regularization parameters α: 10^{-2} (□), 10^{-1} (▽), 10^{0} (×), 10^{1} (△), and 10^{2} (∗).

fixed, then partial treatment around $\varphi = 0$ can reduce this effect.

V. CONCLUSIONS

Sound field control with a circular double-layer of loudspeakers has been experimentally validated. Loudspeakers mounted back-to-back have been used to realize the double-layer of loudspeakers. The experimental results have shown that this system provides an acoustic contrast of more than 30 dB and a normalized spatial error of less than −10 dB below the spatial Nyquist frequency of the outer array (about 392 Hz). Up to 700 Hz, well above the Nyquist frequency, an acoustic contrast of more than 20 dB is obtained. A large degradation of the performance appears at 400 Hz where the distance between the inner and the outer array is half-a-wavelength, and the simulation results have shown that the cancelation between each pair of loudspeakers makes the system sensitive to experimental errors. The experiment on the effect of regularization have shown that the contrast can be improved by about 5 dB below 500 Hz, at the expense of increasing the spatial error.

ACKNOWLEDGMENTS

This research has been supported by the H. C. Ørsted postdoctoral program, and the instruments for the experiments have been provided by the H. C. Ørsted foundation.

[1]M. A. Poletti, F. M. Fazi, and P. A. Nelson, "Sound reproduction systems using fixed-directivity loudspeakers," J. Acoust. Soc. Am. **127**, 3590–3601 (2010).
[2]M. A. Poletti and T. D. Abhayapala, "Interior and exterior sound field control using general two-dimensional first-order sources," J. Acoust. Soc. Am. **129**, 234–244 (2011).
[3]M. A. Poletti, F. M. Fazi, and P. A. Nelson, "Sound reproduction systems using variable-directivity loudspeakers," J. Acoust. Soc. Am. **129**, 1429–1438 (2011).
[4]M. A. Poletti, T. D. Abhayapala, and P. Samarasinghe, "Interior and exterior sound field control using two dimensional higher-order variable-directivity sources," J. Acoust. Soc. Am. **131**, 3814–3823 (2012).
[5]J.-H. Chang and F. Jacobsen, "Sound field control with a circular double-layer of loudspeakers," J. Acoust. Soc. Am. **131**, 4518–4525 (2012).
[6]J.-Y. Park, M.-H. Song, J.-H. Chang, and Y.-H. Kim, "Performance degradation due to transfer function errors in acoustic brightness and contrast control: Sensitivity analysis," in *Proceedings of the 20th International Congress on Acoustics* (2010).
[7]S. J. Elliott, J. Cheer, J.-W. Choi, and Y. Kim, "Robustness and regularization of personal audio systems," IEEE Trans. Audio Speech Lang. Proc. **20**, 2123–2133 (2012).
[8]N. Stefanakis and F. Jacobsen, "Effort variation regularization in sound field reproduction," J. Acoust. Soc. Am. **128**, 740–750 (2010).
[9]T. Betlehem and C. Withers, "Sound field reproduction with energy constraint on loudspeaker weights," IEEE Trans. Audio Speech Lang. Proc. **20**, 2388–2392 (2012).
[10]P.-A. Gauthier and A. Berry, "Adaptive wave field synthesis for active sound field reproduction: Experimental results," J. Acoust. Soc. Am. **123**, 1991–2002 (2008).
[11]F. M. Fazi, P. A. Nelson, J. E. N. Christensen, and J. Seo, "Surround system based on three dimensional sound field reconstruction," in *Proceedings of the 125th Audio Engineering Society Convention*, Paper No. 7555 (2008).
[12]J.-H. Chang, C.-H. Lee, J.-Y. Park, and Y.-H. Kim, "A realization of sound focused personal audio system using acoustic contrast control," J. Acoust. Soc. Am. **125**, 2091–2097 (2009).

Downloaded 16 Apr 2013 to 192.38.67.112. Redistribution subject to ASA license or copyright; see http://asadl.org/terms

[13]W.-H. Cho, J.-G. Lee, and M. M. Boone, "Holographic design of a source array achieving a desired sound field," J. Audio Eng. Soc. **58**, 282–298 (2010).
[14]M. Shin, S. Q. Lee, F. M. Fazi, P. A. Nelson, D. Kim, S. Wang, K. Park, and J. Seo, "Maximization of acoustic energy difference between two spaces," J. Acoust. Soc. Am. **128**, 121–131 (2010).
[15]N. Epain and E. Friot, "Active control of sound inside a sphere via control of the acoustic pressure at the boundary surface," J. Sound Vib. **299**, 587–604 (2007).
[16]IEC International Standard 50 (801), "International electrotechnical vocabulary" (1994).
[17]J. Vanderkooy, "The low-frequency acoustic centre: measurement, theory and application," in *Proceedings of the 128th Audio Engineering Society Convention*, Paper No. 7992 (2010).
[18]A. J. Berkhout, D. de Vries, and P. Vogel, "Acoustic control by wave field synthesis," J. Acoust. Soc. Am. **93**, 2764–2778 (1993).
[19]J.-W. Choi and Y.-H. Kim, "Generation of an acoustically bright zone with an illuminated region using multiple sources," J. Acoust. Soc. Am. **111**, 1695–1700 (2002).
[20]V. A. Morozov, *Methods for Solving Incorrectly Posed Problems* (Springer, New York, 1984), Chap. 26.
[21]D. B. Ward and G. W. Elko, "Effect of loudspeaker position on the robustness of acoustic crosstalk cancellation," IEEE Signal Process. Lett. **6**, 106–108 (1999).
[22]P. C. Hansen, "Analysis of discrete ill-posed problems by means of the L-curve," SIAM Rev. **34**, 561–580 (1992).
[23]P. C. Hansen, *Discrete Inverse Problems: Insight and Algorithms* (SIAM, Philadelphia, 2010), Chaps. 3–4.

Downloaded 16 Apr 2013 to 192.38.67.112. Redistribution subject to ASA license or copyright; see http://asadl.org/terms